Sensitive NADH Detection in a Tumorigenic Cell Line Using a Nano-biosensor based on the Organic Complex Formation

Mahmood H Akhtar, Tanveer A Mir, N.G. Gurudatt, Saeromi Chung, Yoon-Bo Shim

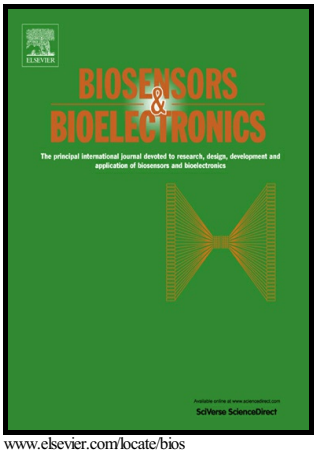

www.elsevier.com/locate/bios

PII: S0956-5663(16)30475-4
DOI: http://dx.doi.org/10.1016/j.bios.2016.05.045
Reference: BIOS8735

To appear in: *Biosensors and Bioelectronic*

Received date: 6 May 2016
Revised date: 11 May 2016
Accepted date: 13 May 2016

Cite this article as: Mahmood H Akhtar, Tanveer A Mir, N.G. Gurudatt, Saeromi Chung and Yoon-Bo Shim, Sensitive NADH Detection in a Tumorigenic Cel Line Using a Nano-biosensor based on the Organic Complex Formation *Biosensors and Bioelectronic,* http://dx.doi.org/10.1016/j.bios.2016.05.045

Sensitive NADH Detection in a Tumorigenic Cell Line Using a Nano-biosensor based on the Organic Complex Formation

*Mahmood H Akhtar, Tanveer A Mir, N. G. Gurudatt, Saeromi Chung, and Yoon-Bo Shim**

Department of Chemistry and Institute of Biophysio Sensor Technology (IBST),

Pusan National University, Busan 46241, South Korea

[*] Corresponding author: Prof. Yoon-Bo Shim

Department of Chemistry and Institute of Bio·Physio Sensor Technology (IBST),

Pusan National University, Busan 46241, South Korea.

E-mail: ybshim@pusan.ac.kr

Tel.: +82-51-510-2244; Fax: +82-51-514-2122.

Abstract:

A robust amperometric sensor for β-nicotinamide adenine dinucleotide (NADH) detection was developed through the organic complex formation with ethylenediaminetetraacetic acid (EDTA) bonded on the polyethylenimine (PEI)/activated graphene oxide (AGO) layer. The EDTA immobilized sensor probe (GCE/AGO/PEI-EDTA) revealed a catalytic property towards NADH oxidation that allows for the highly sensitive electrochemical detection of NADH at a low oxidation potential. Surface characterization demonstrated that the negatively charged AGO acted as nanofillers in the positively charged PEI matrix through the charge interaction. The immobilization of EDTA on the polymer layer provided more surface area for NADH to interact with through the enhanced chemical interlocking between them. We observed the strong interaction between NADH and EDTA on the AGO/PEI layer using a quartz crystal microbalance (QCM), X-ray photoelectron spectroscopy (XPS), and the calculation of the minimized energy for complex formation. The dynamic range of NADH was determined to be between 0.05 μM and 500 μM with a detection limit (LD) of 20.0 ± 1.1nM. The reliability of the developed sensor for biomedical applications was examined by detecting NADH in tumorigenic lung epithelial cells using the standard addition method.

Keywords: NADH sensor, human serum, tumorigenic cells, EDTA, polymer-GO.

1. Introduction

β-Nicotinamide adenine dinucleotide (NADH) is a universal biological molecule found in all living cells, and the functions of this metabolic cofactor have been attributed to the transfer of hydrogen atoms and electrons from one metabolite to another in several intracellular redox reactions, such as glycolysis, the Krebs cycle, and oxidative phosphorylation (Bartlett, 2008). In addition to regulating bioenergetics and maintaining mitochondrial function, the NADH-NAD^+ redox couple plays critical roles in multiple biological reactions catalyzed by over 300 NADH-dependent dehydrogenases (Zhao et al., 2011). The regulation of the intracellular concentration ratio of NADH and NAD^+ is also essential for all cells to maintain numerous vital processes, and its changes have been associated with alteration in energy metabolism under various pathophysiological conditions, such as aging, cancer, Parkinson's disease, diabetes, and epilepsy (Ying et al., 2011; Lin et al., 2003; Allison et al., 2014; Belenky et al., 2007). Thus, it is important to develop a robust biosensor for NADH or NAD^+ detection.

In view of the importance of NADH monitoring, several methods to detect NADH have been developed employing capillary electrophoresis, high performance liquid chromatography, spectroscopy, and enzymatic cycling (Bartlett, 2008; Álvarez et al., 2000; Kasischke et al., 2011; Xie et al., 2011; Zhou et al., 2011). Although these techniques allow the determination of NADH, they are complicated, time consuming, and require sophisticated equipment. Alternatively, the electrochemical method is advantageous and frequently used, because it is considered to be selective, facile, reproducible, and has the ability to be miniaturized for point of care applications. However, there are still many challenges in the electrochemical detection of NADH due to its high polarization potential and electrode fouling effects, which results in the adsorption of oxidation products of NADH. There is also interference from easily oxidizable species present in real samples. To

improve the sensitivity and the selectivity of the sensor, considerable efforts have been devoted to modify the probe with a variety of biomimetic, metallic and non-metallic materials, which can effectively overcome kinetic barriers for the oxidation of NADH (Li et al., 2015; Omar et al., 2016; Radoi et al., 2009; Lee et al., 2010). Despite the good performances of those electrochemical sensors, there are still several shortcomings in their sensitivities, reproducibilities, and fouling effects. Thus, we tried to develop a new NADH sensor through the complex formation between NADH and a probe molecule, where EDTA was a good candidate, because it has the many carboxylic acid and amine groups that can interact with NADH molecule through the hydrogen bonding.

A stable polycation is one of good substrate to immobilize the EDTA molecule, because they can improve the electrocatalytic activity and the stability by forming a composite layer with nanocatalytic materials. Among these polycations including poly 3'-(2-aminopyrimidyl)-2,2':5',2''-terthiophene (APT), poly (amidoamine) (PAA), and polyethylene imine (PEI) (Naveen et al., 2015; Samal et al., 2012), PEI has attracted significant attention in the analytical, sensing, and biomedical fields due to its solubility in water, neutral pH buffering capacity, and rich amine groups. Hence, we examined PEI as a substrate polymer material, after enhancing the electrically conductivity using activated graphene that was stably composited with the PEI. Graphene oxide (GO) was further activated (AGO) with sonication offering a rich surface chemistry to enhance the performance of the sensor probe. GO presents highly reactive oxygen functionalities on its edge sites (Gong, 2013), demonstrating that GO is a good nanofiller for positively charged polymer layers (Stankovich et al., 2006). Hence, we expect that the immobilization of EDTA on the PEI/AGO layer provides an enhanced selectivity and sensitivity of the sensor probe by improving the conductivity and the interaction with NADH.

In the present work, we constructed a novel EDTA-modified sensor probe (AGO/PEI-EDTA). The formation of the nanocomposite of probe materials was characterized using field emission scanning electron microscopy (FE-SEM), Raman spectroscopy, and XPS. The complex formation between NADH and EDTA was confirmed by the calculation of the minimized energy, XPS, and QCM. The analytical performance of the proposed sensor was evaluated using cyclic voltammetery (CV), chronoamperometery, and EIS. Finally, to evaluate the reliability of the sensor, NADH was detected in real samples. To the best of our knowledge, this is the first report in which EDTA has been utilized to develop a sensor probe for the detection of NADH directly in tumorigenic cell line and human serum.

2. Materials and methods

2.1 Reagents and instruments

β-nicotinamide adenine dinucleotide (NADH), polyethylenimine (PEI), dopamine (DA), ascorbic acid (AA), uric acid (UA), catechol (CA), graphite, sulfuric acid (98%), aluminum chloride, hydrogen peroxide (H_2O_2), ethylenediaminetetraacetic acid (EDTA), potassium permanganate, sodium phosphate dibasic, sodium phosphate monobasic, HCl, $K_3[Fe(CN)_6]^{4-/-3}$, $[Ru(NH_3)_6]Cl_3$, $KMnO_4$, $NaNO_3$, Dulbecco's modified Eagle medium (DMEM), fetal bovine serum (FBS), trypsin-EDTA, penicillin/streptomycin, PBS solution, human serum, and the celLytic^{TM} solution were obtained from Sigma-Aldrich (USA). A549 cells were obtained from the Korean Cell Bank. All aqueous solutions were prepared in ultra-pure water obtained from a Milli-Q water purification system (18M Ω cm). All electrochemical measurements were performed at room temperature using a conventional electrochemical cell system. Modified glassy carbon with a geometric area of 0.07 cm^2, an Ag/AgCl electrode (in saturated KCl), and a platinum (Pt.) wire were used as the working, reference, and counter electrodes, respectively. CVs were recorded using a Kosentech PT-1 model and an EG & G

PAR 273A model galvanostat. The impedance spectra were measured with the EG&G Princeton Applied Research, PARSTAT 2630. The morphology of the composite was confirmed by FE-SEM images, and XPS experiments were performed in KBSI (Busan) using a VG Scientific ESCA Lab 250 XPS spectrometer coupled with a monochromatic Al Kα source with charge compensation. For XPS analysis, we used XPSPEAK41 software and the peaks were fitted using the linear model as background subtraction. Raman spectroscopy was performed using a WITec alpha 300 Raman microscope (WITec, Ulm, Germany) equipped with an UHTS-300 spectrometer with an excitation wavelength of 531.9 nm. QCM experiments were performed using a SEIKO EG&G model QCA 917 and a PAR model 263A potentiostat/ galvanostat (USA).

2.2 Activation of GO

Graphene oxide (GO) was freshly prepared by following the reported method (Gong, 2013). Activation of GO (AGO) was performed by sonication for a certain amount of time (0 -15 hrs). It has been reported that edge plane defects could enhance the conductivity of GO through facile electron transfer (Yuanet al., 2013). CV was employed in the solution phase, and the maximum NADH response current was observed at 12 hrs. After12 hrs, the current change was insignificant (data not shown).

2.3 Preparation of sensor probes

The GC electrode was cleaned using wet soft polishing cloth with alumina powders (0.5 and 0.03 mm, successively). After rinsing with water in each polishing step, the electrode was subjected to sonication in ethanol and water for 1 min to remove the adsorbed residual alumina particles and was then dried at ambient conditions. To prepare the AGO/PEI nanocomposite, first 0.5mg/ml GO and PEI (50 wt. %) were dispersed with the aid of ultrasonic agitation for 12 hrs and then, the AGO/PEI composite was ready for the subsequent experiments. The electrode was modified by drop casting 10 µl of the AGO/PEI

nanocomposite on the GC electrode surface and allowing it to dry at room temperature. Subsequently, the modified electrode was immersed in EDC/NHS solution containing EDTA (10 mM) for 12 hrs for activation of carboxylic acid groups and immobilization of EDTA onto the GCE/AGO/PEI layer. Finally, the GCE/AGO/PEI-EDTA sensor probe was fabricated, and used for the NADH analysis.

2.4 Preparation of tumorigenic lung epithelial (A549) cell samples

The human tumorigenic lung epithelial (A549) cells were maintained in T75 cell culture flasks containing Dulbecco's modified Eagle medium (Sigma) supplemented with 10% fetal bovine serum (Sigma) and 100 units/ml of penicillin/streptomycin (Gibco). The cells were maintained in an incubator at 37°C in a 95% humidified atmosphere and 5% carbon dioxide. The cells were passaged every 5-6 days, and the medium was renewed every two days. For the extraction of NADH from cultured cells into the solution to be measured, the cultured cells were washed with sterilized PBS two or three times to remove any remaining growth media, and then they were lysed by adding 300 µL of CelLytic^{TM} solution. For control experiments, cell sample without treating with the CelLytic^{TM} solution and only with the CelLytic^{TM} solution were used.

3. Results and Discussion

The schematic representation of the construction of the GCE/AGO/PEI-EDTA composite layer as well as, NADH detection are shown in Scheme 1. Prior to the formation of the composite layer of PEI and GO, further activation of GO (AGO) by sonication was expected to provide more edges, resulting in improvement in the performance of GO. After the formation of the AGO and PEI composite, EDTA, an anionic molecule containing four carboxylic groups, can be stably modified on the PEI/AGO surface, to exploit the complexation with NADH or NAD^+. First, the electrode was modified by casting 10 µl of

the AGO/PEI suspension onto the GC electrode surface, and then the organic nano composite was dried at room temperature. The GCE/AGO/PEI modified electrode was incubated in an EDC/NHS solution containing EDTA (10 mM) for 12 hrs to form the amide bond between NH_2 groups of PEI and –COOH groups of EDTA. The final sensor probe of GCE/AGO/PEI-EDTA was thus fabricated and subsequently characterized by surface analysis methods.

3.1 Surface characterization of the sensor probe

At first, to confirm the successful fabrication of the sensor probe, XPS analysis was performed to elucidate the immobilization of EDTA on the GCE/AGO/PEI layer. Figure 1 shows the survey and the deconvoluted spectra for (i) GCE/AGO (ii) GCE/AGO/PEI and (iii) GCE/AGO/PEI-EDTA modified surfaces. A deconvoluted C1s spectrum for AGO/PEI as shown in Figure 1 b (ii), revealed the presence of C-C/C=C, C-O/C-O-C, and N-C=O peaks at 284.3, 285, and 285.4 eV, respectively. In the deconvoluted C1s spectrum for GCE/AGO/PEI-EDTA as shown in Figure 1 b (iii), the C-C, and C-O peaks were shifted to higher binding energy values at 284.5, and 284.8 eV. Though, the N-C=O peak was remained on the same position at 285.3eV (Fig. 1 b (iii)), but the intensity of the peak was increased. Moreover, the C1s peak at 287.82 eV corresponding to O-C=O of the EDTA is not observed at the only AGO/PEI layer without EDTA. However, the peak corresponding the C1s spectrum of AGO appeared at 288.85 eV (Figure 1 b (i)), which disappeared after covering of the PEI on the AGO layer. This confirms that the C1s peak at 287.82 eV is indeed for the EDTA layer. The deconvoluted N1s spectrum for the GCE/AGO/PEI as shown in Figure 1 c (i), illustrated two peaks for $–NH_2$ and –NH at 398.25 eV and 398.55 eV, respectively. After the immobilization of EDTA (Figure 1 c (ii)), the peaks of $–NH_2$, –NH were shifted to higher energy values at 398.62 and 398.65 eV, respectively, as a result of a protonated primary amine nitrogen, $–NH_2^+–$ (Naveen et al., 2015). Moreover, a C–N peak appeared due to the

hydrogen bonding between –NH_2 groups of PEI and –COOH groups of EDTA. The O1s spectra of AGO/PEI modified GCE surface as shown in Fig. 1 d (ii) illustrated two peaks at 530.35 eV and 531.90eV for O-C=O and C-N=O, respectively. After the immobilization of NADH, the C-N=O peak as shown in Fig. 1 d (iii) shifted to a lower energy value indicating the higher electrostatic attraction. Also, another peak appeared at 535.15 eV (Fig. 1 d (iii)) corresponding to the C-O bond formation due to the added–COOH groups of EDTA, thus showing the successful immobilization of EDTA. These XPS data adequately confirm the successful attachment of PEI as well as EDTA immobilization.

The surface morphologies of the sensor probe were examined by FE-SEM. Figure S1 (a-b) shows the images of (a) GCE/AGO/PEI and (b) GCE/AGO/PEI-EDTA layers of the sensor probe. The AGO/PEI layer on the GCE displays a rough morphology after sonication for a given amount of time. This indicates that the sheet structure of GO is well maintained even after the mixing of GO and PEI, and it also provides a large surface area, which helps in forming more active sites on the electrode surface. The GCE/AGO/PEI-EDTA layer exhibits small clusters, which are due to the aggregation of EDTA by hydrogen bonding on the PEI layer, indicating successful fabrication of the GCE/AGO/PEI-EDTA layer.

Prior to modifying the sensor probe, GO was activated by sonication to attain greater edge surface area. The edge and basal plane defects in carbonaceous materials can be confirmed by Raman spectroscopic peaks, which are characterized as D and G bands. Previous reports suggest that the intensity ratio of (D/G) is often used as a means of determining edge and basal planes or overall stacking behavior (Yuanet al., 2013). The intensity ratio of (D/G) was increased by upto 12 hrs of sonication of GO, and it remained unaffected at sonication times over 12 hrs (Figure S2). This could be attributed to the formation of additional edge defects, which is termed activated GO.

CV and impedance spectroscopy were employed to characterize the surface conditions of the bare and GCE/AGO/PEI-EDTA sensor probes in 4 mM $[Fe(CN)_6]^{3-}$ and $[Ru(NH_3)_6]^{3+}$solutions (Figure S3). A well-defined redox peak for the$[Fe(CN)_6]^{4-/3-}$ couple was observed for the bare electrode, while no obvious peak for the sensor probe was observed (Figure S3 a (i, ii)). However, a well-defined peak was observed for the final sensor probe in the $[Ru(NH_3)_6]^{3+}$solution (Figure S3 b (i, ii)), while the redox peak at the bare electrode was smaller than that of the final sensor surface. Additionally, impedance spectroscopy was performed at an open circuit voltage to monitor resistance variations at bare and sensor probe surfaces. The Rct values for the bare and the sensor probes in a $[Fe(CN)_6]^{3-}$ solution were observed to be 0.6 kΩ, and 7.9 kΩ, respectively, (Fig. S3 c (i, ii)), while Rct values for the bare GC and sensor probe were 45.2 kΩ, and 4.6 kΩ, respectively, in the $[Ru(NH_3)_6]^{3+}$ solution (Fig. S3 d (i, ii)). These results show that the sensor surface is covered with negatively charged EDTA molecules.

3.2 Interaction between the sensor probe and NADH

To observe the sensing ability of the sensor probe towards NADH, CVs were recorded at bare GCE, GCE/AGO, GCE/AGO/PEI and GCE/AGO/PEI-EDTA layers in PBS at a neutral pH containing 500 μM NADH as shown in Figure 2 (a). As shown in the figure, the anodic peak of NADH was enhanced at the GCE/AGO/PEI-EDTA modified surface due to the complex formation between EDTA and NADH molecules through the hydrogen bonding. We investigated the mechanism using the scan rate dependency test. The response current was proportional to the square root of scan rate (Fig. S4), indicating that the diffusion controlled process was involved in the NADH oxidation at the sensor probe. The linear relationship between the current vs. NADH concentrations from 0.5 μM to 500 μM was observed at the GCE/AGO/PEI-EDTA with a correlation coefficient of 0.998 as shown in inset (Fig.2 (b)), demonstrating the excellent sensing performance of the proposed sensor probe.

Furthermore, QCM analysis was performed to estimate the captured quantity of NADH by the interaction of NADH with AGO, PEI, AGO/PEI and AGO/PEI-EDTA as shown in Figure 2 (c). The interaction of NADH with AGO, PEI, and AGO/PEI (Fig.2 c (i, ii, iii)) was observed with an insignificant frequency change of (Δf = 9.4, 19.7, 35 Hz) and the estimated amount of physically adsorbed NADH was found to be 8.6, 18.3, and 34.71 ng, respectively, based on a previously defined equation (Lee et al., 2010). However, a significant change in the frequency (Δf = 270 Hz) was observed for the AGO/PEI-EDTA/NADH interaction as shown in Fig.2 c (iv), which corresponds to a NADH mass change (Δm) of 265.57 ng. These results provide evidence for the high interaction of NADH with the EDTA layer, and hence show the strong interaction as compared with the other layers.

To support our hypothesis about the complex formation between EDTA and NADH, at first, their interaction was predicted by evaluating the calculation of the minimized energy values using Chem3D pro 12.0, and it is suggested that the interaction occurred in three different possible ways as shown in Figure 3 (a-c.). Fig.3 (a) shows the interaction of two carboxylic acid groups of EDTA with two hydroxyl groups and a phosphate group of NADH through three hydrogen bonds, showing a minimized energy value of -56.2301 kcal/mol. Fig. 3 (b) depicts the interaction of the two carboxylic acid groups of EDTA are with two hydroxyl groups, a phosphate group, and an amine group of NADH through four hydrogen bonds with a minimized energy value of -47.7688 kcal/mol. Fig. 3 (c) gives the minimized energy value of -43.0798 kcal/mol through the formation of four hydrogen bonds. As shown in Figure 3 (a), the complex formed at the minimized energy value of -56.2301 kcal/mol, is more favorable compared to the others due to less steric hindrance.

In addition, XPS analysis was performed in detail to verify the complexation between EDTA and the NADH and confirmed the binding energy shift of P-O, C=O, and C=N bonds after the interaction between them. Fig. 3 (d) shows the survey spectra obtained for

AGO/PEI-EDTA (i) before and (ii) after the NADH interaction with the probe. As shown in Fig. 3 (d), a new phosphorus peak (P2p) appeared after the interaction of NADH with the probe molecule which did not exist before. The additional evaluation for the interaction of NADH with the EDTA modified sensor probe was performed using the deconvoluted spectra of C1s, N1s, and O1s as shown in Fig. 3 (e-g). The C1s spectrum of AGO/PEI-EDTA (Fig. 3 (e)) shows four peaks at 284.35, 284.5, 285.3, and 287.8 eV, which correspond to C-C, C-O or C-N, N-C=O, and O=C-O$^-$ bonds of the probe molecules, respectively. By the interaction between NADH and EDTA molecules, the C-O (or C-N) and N-C=O peaks were shifted from 284.5 and 285.3 eV to 284.9 and 285.9 eV, respectively, and the $^-$O-C=O peak was also slightly shifted from 287.8 eV to 286.85 eV as shown in Fig. 3 e (ii). The N1s peaks for AGO/PEI/EDTA appeared at 398.6, 398.95, and 399.8 eV (Fig.3 (f-i)) corresponding to -NH_2, -NH, and N-C, respectively. The -NH_2 and -NH peaks of the EDTA modified probe were shifted from 398.6 and 398.95 eV to 398.68 and 399.35 eV due to their involvement in the interaction as shown in Fig. 3 (b). After the interaction between NADH and EDTA, the N-C, N=C bonds of the NADH molecule leads to a shift in the peak at 399.8 eV to 400.65 eV. The O1s spectra of the EDTA modified sensor contains three peaks at 535.16 (C-O), 531.72 (O=C-N), and 530.94 eV (O=C-O) as shown in Fig. 3 (g-i). The interaction of NADH with the EDTA leads to a decrease of the C-O bond energy of EDTA. Therefore, the O1s binding energies for all three peaks were shifted from 535.16, 531.72 and 530.94 eV to 535.7, 531.85, and 531 eV, respectively. Additionally, a new peak appeared at 533.0 eV corresponding to the P-O bond of NADH by the successful interaction between NADH and the EDTA probe. These results are in agreement with the simulated energy diagrams Fig. 3 (a-c). Accordingly, the successful complex formation between EDTA and NADH was demonstrated.

3.3 Optimization of the analytical parameters and interference studies

To achieve optimal sensitivity, analytical parameters for the detection of NADH with the proposed probe were optimized in terms of the GO-activation time, applied potential, pH, and EDTA concentrations. The sensor probe showed an enhanced response with increasing GO-activation time (in terms of sonication), and the maximum response was observed at 12 hrs. Thus, 12 hrs was chosen as the optimal activation time (Figure S5 (a)). The effect of the applied potential on the detection of NADH was also examined between 0.15 V to 0.45 V. The response current elevated as the applied potential increased from 0.15 V to 0.4 V. The maximum response was observed at 0.4 V, and no significant increase in the signal was observed over 0.4 V (Figure S5 (b)). Hence, subsequent measurements were performed at this potential. The effect of the pH of the solution being measured on the response was investigated at the range of 5.0-8.0. The response current steadily increased from a pH of 5.0 to a pH of 7.4, it then decreased over 7.4. The interaction between EDTA-NADH provided the maximum current response at this pH. Thus, pH 7.4 was selected as the optimal pH (Figure S5 (c)), and subsequent experiments were performed at this pH. In addition, the effect of the amount of EDTA attached on the sensor surface was also examined from 2 mM to 12 mM. The response current gradually increased as the concentration of EDTA increased from 2.0 to 10 mM, and it reached a steady state over 10 mM EDTA. No increase in the signal was observed over this concentration due to the saturation. Thus, 10 mM EDTA was chosen for subsequent experiments (Figure S5 (d)).

To assess the possibility of interference from common biomolecules on the proposed biosensor, chronoamperometery was recorded in the presence of ascorbic acid (AA), acetaminophen (AP), uric acid (UA), catechol (CA), and dopamine (DA). As shown in Fig. 4 (a), the sensor exhibited a clear amperometric response towards NADH (50 μM), while no-noticeable signals were observed for AA (0.5 mM), AP (0.5 mM), UA (0.5 mM), CA (0.5 mM), and DA (0.5 mM). Although NADH is not a positively charged molecule, but as a

result of the hydrogen bond formation between EDTA and NADH, the sensor showed an excellent response to NADH. The diffusion of other charged species without enough interaction sites for strong hydrogen bond formation with EDTA will be blocked at the modified sensor probe surface. Therefore, no detectable response was observed for AA, AP, UA, CA, and DA when they coexist in the same PBS solution. These results indicate that the proposed sensor can be used for the selective detection of NADH without interference from common molecules in body fluids.

3.4 Calibration plot, reproducibility and stability

Under the optimized conditions, amperometery was performed using the GCE/AGO/PEI-EDTA sensor to detect NADH. Figure 4 (b) shows the subsequent amperometric response of the sensor to the successive additions of NADH. A well defined response curve was observed upon each successive addition of NADH solution, and the calibration plot is linearly proportional to the NADH concentration throughout the range of 0.05 μM to 500 μM (inset). The linear regression equation of the calibration plot is expressed as follows: *I*p (μA) = 0.0169 (±0.004) + 0.0013 (±0.002) [NADH][μM], with a correlation coefficient of 0.994 (RSD <4.1%, 95% confidence level, k=3, n=5). The detection limit was calculated based on 3s (where s is the standard deviation of the blank solution, n=10), and it was determined to be 20.0 ±1.1 nM. The performance of constructed NADH biosensor was compared with other reported works (Table S1), generally, the electrochemical methods exhibit a LD ranging from 0.1 to 250 μM. The spectroscopic techniques such as electrochemiluminescence, and UV–vis. photometry show LD 5 fM, and 15.6 μM, respectively. In the present study as compared to previous amperometric methods, the LD was calculated to be 0.02 μM which is about 5 times more sensitive.

To demonstrate the reproducibility of the proposed sensor, five parallel measurements were performedin PBS containing 200 μM of NADH. A relative standard deviation

(RSD/coefficient of variation) of 2.39 % was achieved in the same surface area modified with GCE/AGO/PEI-EDTA, which clearly shows that the sensor is remarkably reproducible. Five different GCE/AGO/PEI-EDTA probes were also tested in a 200 µM NADH solution to examine how the response current differs between electrodes. The variation in the current was found 3.16% which indicates good sensor to sensor reproducibility. The accuracy of the sensor was also verified through the standard addition method (Table S2). The storage stability of the sensor probe was also evaluated at regular time intervals (in 200 µM NADH solution once a week) for a duration of eight weeks. When the sensor probe was stored at 4ºC for eight weeks, the sensor maintained 92 % of its initial response. These results indicate that the presented sensor possesses satisfactory stability, accuracy, and reusability.

3.5 Analysis of NADH in human serum and cultured tumorigenic cells

To assess the practical applicability of the proposed sensor in complex biological matrices, the NADH concentration was analyzed in human serum and tumorigenic lung cell samples. For serum sample analysis, chronoamperometric measurements of the five folds diluted human serum were performed. The serum did not exhibit any chronoamperometric response, indicating that the amount of NADH present in the serum was less than the detection limit of sensor or it was not present in the sample. Afterwards, known amounts of a standard NADH solution were spiked into the serum, and the amperometric responses were recorded. As shown in Figure 5 (a), the response and a corresponding calibration plot were obtained after exposing the sensor probe to the human serum sample into which different amounts of a standard solution of NADH were injected. As depicted, the amperometric response increased with increasing NADH concentrations, and a linear regression equation could be expressed as Ip (µA) = 102.2 (±0.003) + 318.75 (±0.016) [NADH][µM], with a correlation coefficient of 0.996. The amount of NADH in the serum sample was determined

by the standard addition method (Table S2) and recoveries were observed in the range of 98.6–100.4% (RSD < 5%, n=5).

Additionally, we investigated the biomedical application of the proposed sensor using tumorigenic cell samples. To extract NADH from cells, cultured A549 (3.0 x10^6 cells/ml) cells were first exposed to CelLytic^{TM} solution and then the lysed cell suspension was added to the solution being measured (0.1 M PBS, pH = 7.4). The amount of NADH in the lysed cell sample was determined by the standard addition method, and recoveries were observed in the range of 97.8–100.7% (RSD < 5%, n=5) (Table S2). To further validate the results, lysed cell samples were spiked with different concentrations of NADH, and the amperometric responses were obtained (Figure 5 (b)). As shown in the figure, the amperometric response increases with increasing NADH concentrations, and it shows a concentration level 380 nM of NADH in the tumorigenic cell line**.** A linear regression equation can be expressed as follows: *I*p (μA) = 0.143 (±0.003) + 0.3794 (±0.005) [NADH][μM], with a correlation coefficient of 0.999. These results clearly show that the proposed sensing system for the detection of NADH in spiked human serum and tumorigenic cell samples is considered acceptable, and hence, its promising analytical performance towards complex biological sample analysis has been demonstrated.

4. Conclusions

In this study, a simple, highly sensitive, and selective biosensor was successfully developed for the detection of NADH through the formation of complex with an EDTA probe molecule. The sensor probe was characterized by FE-SEM, Raman spectroscopy, XPS, QCM, and electrochemical methods. The complex formation between NADH and EDTA molecules was confirmed by estimating the minimized energy, XPS, and QCM. The current responses of the sensor toward negatively charged interfering species such as ascorbic acid, uric acid

and catecholamine were remarkably eliminated. The proposed sensor was successfully applied to detect NADH in human serum and tumorigenic cell samples. The analytical performance of the proposed sensor for the detection of NADH was excellent in terms of mitigating the over potential, resistance to fouling, sensitivity, selectivity, and reproducibility. The results indicate that the proposed sensor holds considerable promise for various biomedical applications and can be applied in the monitoring of the NADH level in clinical analyses, toxicity tests, and pharmacological evaluations.

Acknowledgement

This work was supported by the researcher program from National Research Foundation of Korea (NRF) grant funded by the Korea government (MSIP) (No, 2015R1A2A1A13027762).

References

Allison, S. J., Knight, J. R. P., Granchi, C., Rani, R., Minutolo, F., Milner, J., Phillips, R. M., 2014. Oncogene. 3, 1-11.

Álvarez-González, M. I., Saidman, S. B., Lobo-Castañón, M. J., Miranda-Ordieres, A. J., Tuñón-Blanco, P., 2000. Anal. Chem.72, 520-527.

Bartlett, P.N., 2008. Bioelectrochemistry: fundamentals, experimental techniques and applications. John Wiley & Sons.

Belenky, P., Bogan, K. L., Brenner, C. 2007. Trends Biochem. Sci. 32, 12-19.

Gong, L. R. (Eds.), 2013. New Progress on Graphene Research; In Tech publishing Co.

Kasischke, K.A., Lambert, E.M., Panepento, B., Sun, A., Gelbard, H.A., Burgess, R.W., Foster, T.H., Nedergaard, M., 2011. J. Cerebr. Blood F Met. 31, 68-81.

Lee, K.-S., Won, M.-S., Noh, H.-B., Shim, Y.-B., 2010. Biomaterials 31, 7827-7835.

Li, Z., Su, W., Liu, S., Ding, X. 2015. Biosens. Bioelectron. 69, 287-293.

Lin, S. J., Guarente, L., 2003. Curr. Opin. Cell Biol. 15, 241-246.

Naveen, M. H., Noh, H. -B., Al Hossain, M. S., Kim, J. H., Shim, Y.-B., 2015. J. Mater. Chem. A3, 5426-5433.

Omar, F. S., Duraisamy, N., Ramesh, K., Ramesh, S. 2016. Biosens. Bioelectron. 79, 763-775.

Radoi, A., Compagnone, D. 2009. Bioelectrochemistry, 76, 126-134.

Samal, S. K., Dash, M., Van V. S., Kaplan, D. L., Chiellini, E., Van B. C., Dubruel, P., 2012. Chem. Soc. Rev. 41, 7147-7194.

Shan, C., Yang, H., Han, D., Zhang, Q., Ivaska, A., Niu, L., 2010. Biosens. Bioelectron. 25, 1504-1508.

Shalini, J., Sankaran, K. J., Chen, H. C., Lee, C. Y., Tai, N. H., Lin, I. N. 2014. Analyst 139, 778-785.

Stankovich, S., Dikin, D. A., Dommett, G. H., Kohlhaas, K. M., Zimney, E. J., Stach, E. A., Ruoff, R. S. 2006. Nature, 442, 282-286.

Xie, W., Xu, A., Yeung, E. S. 2009. Anal. Chem. 81, 1280-1284.

Ying, W., 2008. Antioxid. Redox Sign. 10, 179–206.

Yuan, W., Zhou, Y., Li, Y., Li, C., Peng, H., Zhang, J., Shi, G., 2013. Sci. Rep. 3, 2248.

Zhao, Y., Jin, J., Hu, Q., Zhou, H. M., Yi, J., Yu, Z., Loscalzo, J., 2011. Cell Metab. 14, 555-566

Zhou, Y., Xu, Z., Yoon, J. 2011. Chem. Soc. Rev. 40, 2222-2235.

Figure captions

Scheme 1. Schematic representation of the fabrication steps of the GCE/AGO/PEI-EDTA sensor probe.

Figure 1: (a) XPS survey spectra of (i) AGO, (ii) AGO/PEI and (iii) AGO/PEI-EDTA. (b-d) shows the deconvoluted peaks of C1s of (i, ii, and iii), N1s, and O1s for (ii) and (iii).

Figure 2: (a) CVs obtained for a 500 μM NADH solution with (i) bare GCE, (ii) GCE/AGO, (iii) GCE/AGO/PEI and (iv) GCE/AGO/PEI-EDTA surfaces. (b) Linear calibration plot of current vs. NADH concentrations at GCE/AGO/PEI-EDTA sensor probe. (c) Shows the QCM reponses of (i) AGO, (ii) PEI, (iii) AGO/PEI, and AGO/PEI-EDTA with NADH, respectively.

Figure 3: (a-c) The minimized energy diagrams depicting the complex formation between NADH and EDTA through hydrogen bonding. (d) XPS survey spectra of (i) GCE/AGO/PEI-EDTA sensor probe, and (ii) after the interaction of NADH with the probe. (e) The deconvoluted peaks of C1s for (i) and (ii) respectively. (f) The deconvoluted peaks of N1s, and (g) O1s for (i) and (ii) respectively.

Figure 4: (a) Chronoamperometric response of the GCE/AGO/PEI-EDTA sensor probe containing 50 μM NADH in the presence of potentially interfering molecules with the

concentration of 0.5 mM (AA, AP, UA, CA, and DA). (b) Amperometric response obtained at the GCE/AGO/PEI-EDTA probe for successive additions of NADH into the PBS solution.

Figure 5: (a) Standard addition plot and amperometric responses obtained with GCE/AGO/PEI-EDTA for different volumes of spiked NADH in the serum sample (b) Standard addition plot and amperometric responses obtained with the GCE/AGO/PEI-EDTA sensor probe for different volumes of spiked NADH in the tumorigenic cell sample.

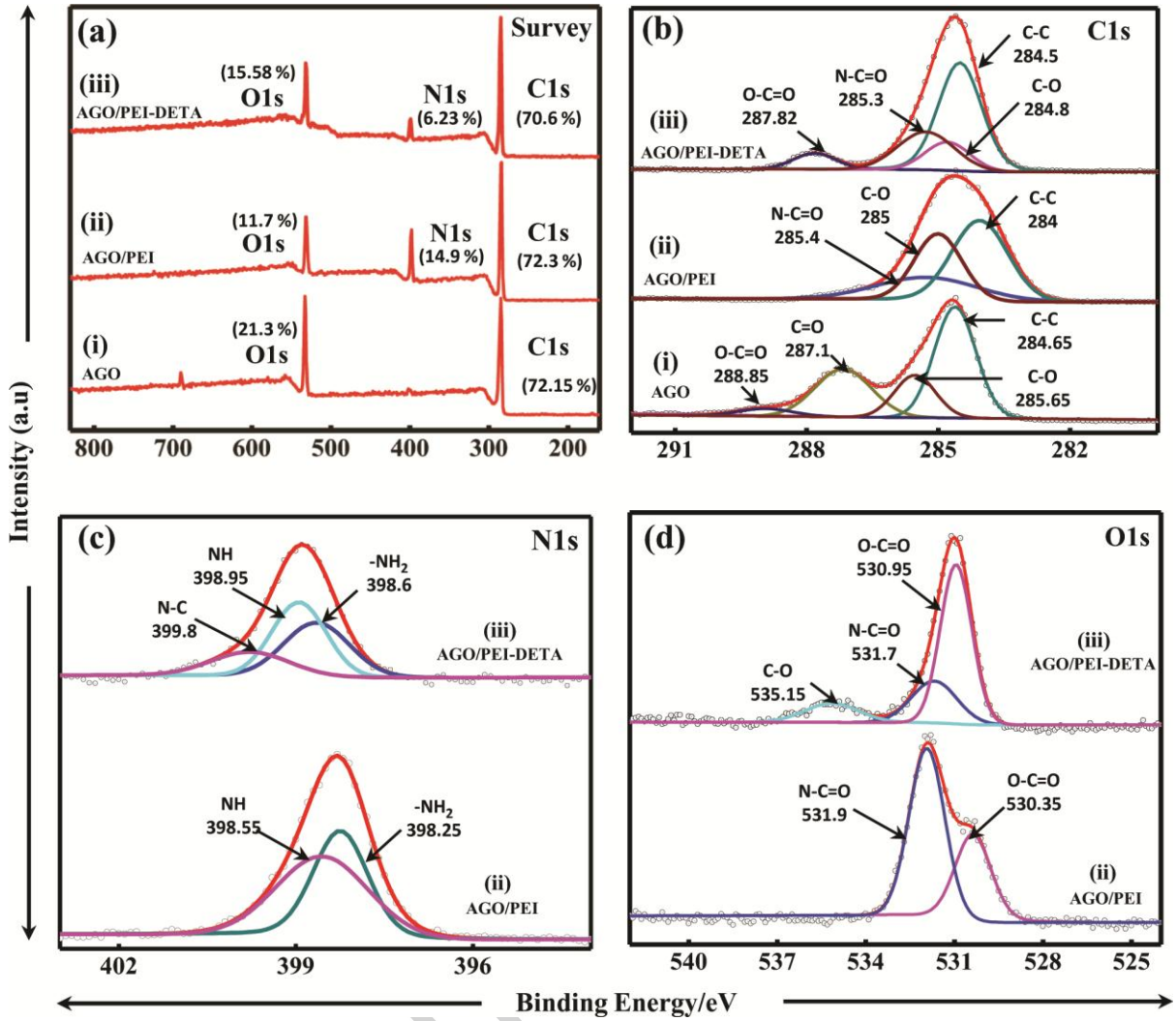

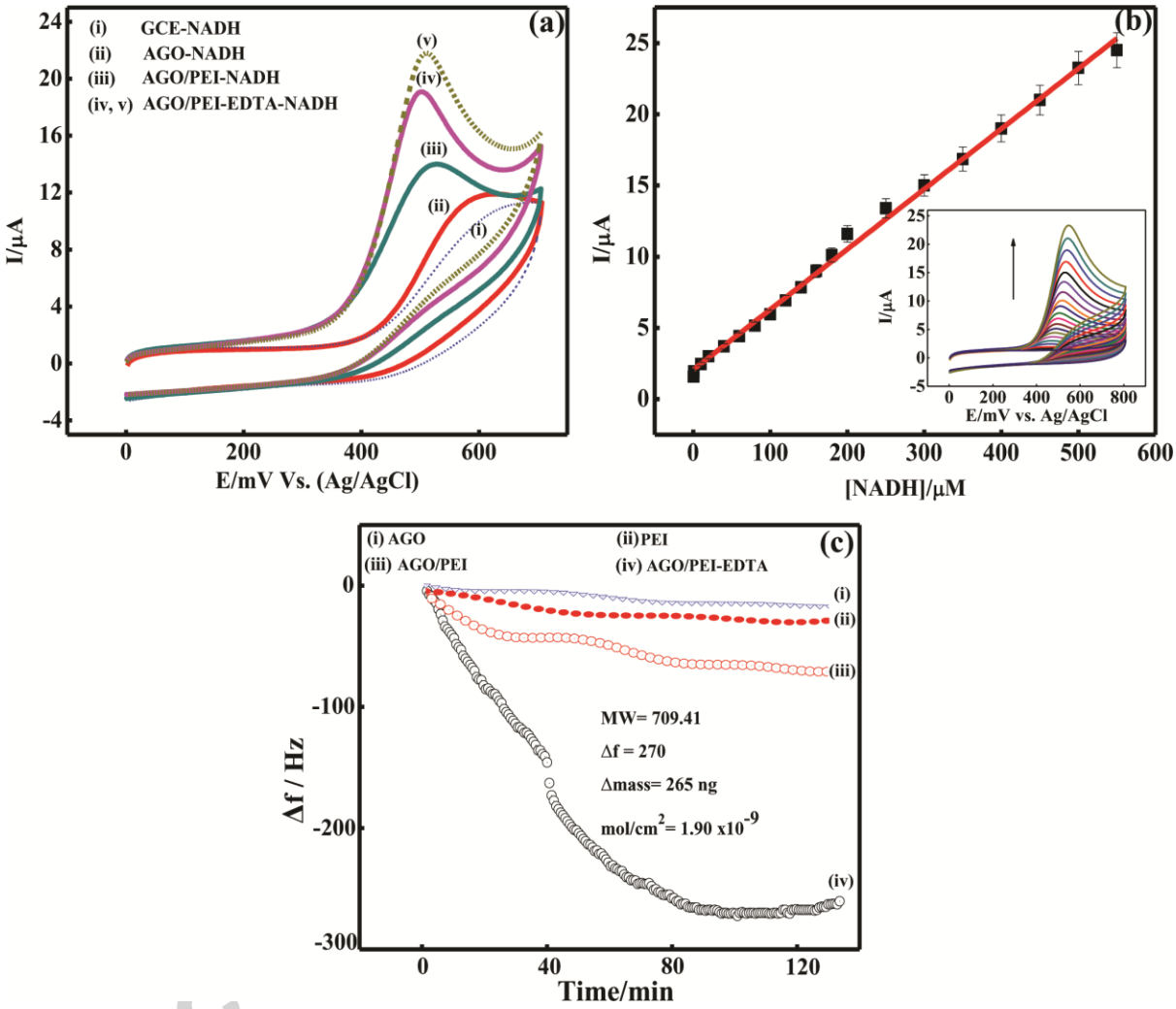
(a)
(i) GCE-NADH
(ii) AGO-NADH
(iii) AGO/PEI-NADH
(iv, v) AGO/PEI-EDTA-NADH
I/μA
E/mV Vs. (Ag/AgCl)
(b)
I/μA
[NADH]/μM
E/mV vs. Ag/AgCl
(c)
(i) AGO
(ii) PEI
(iii) AGO/PEI
(iv) AGO/PEI-EDTA
MW= 709.41
Δf = 270
Δmass= 265 ng
mol/cm2= 1.90 x10-9
Δf / Hz
Time/min

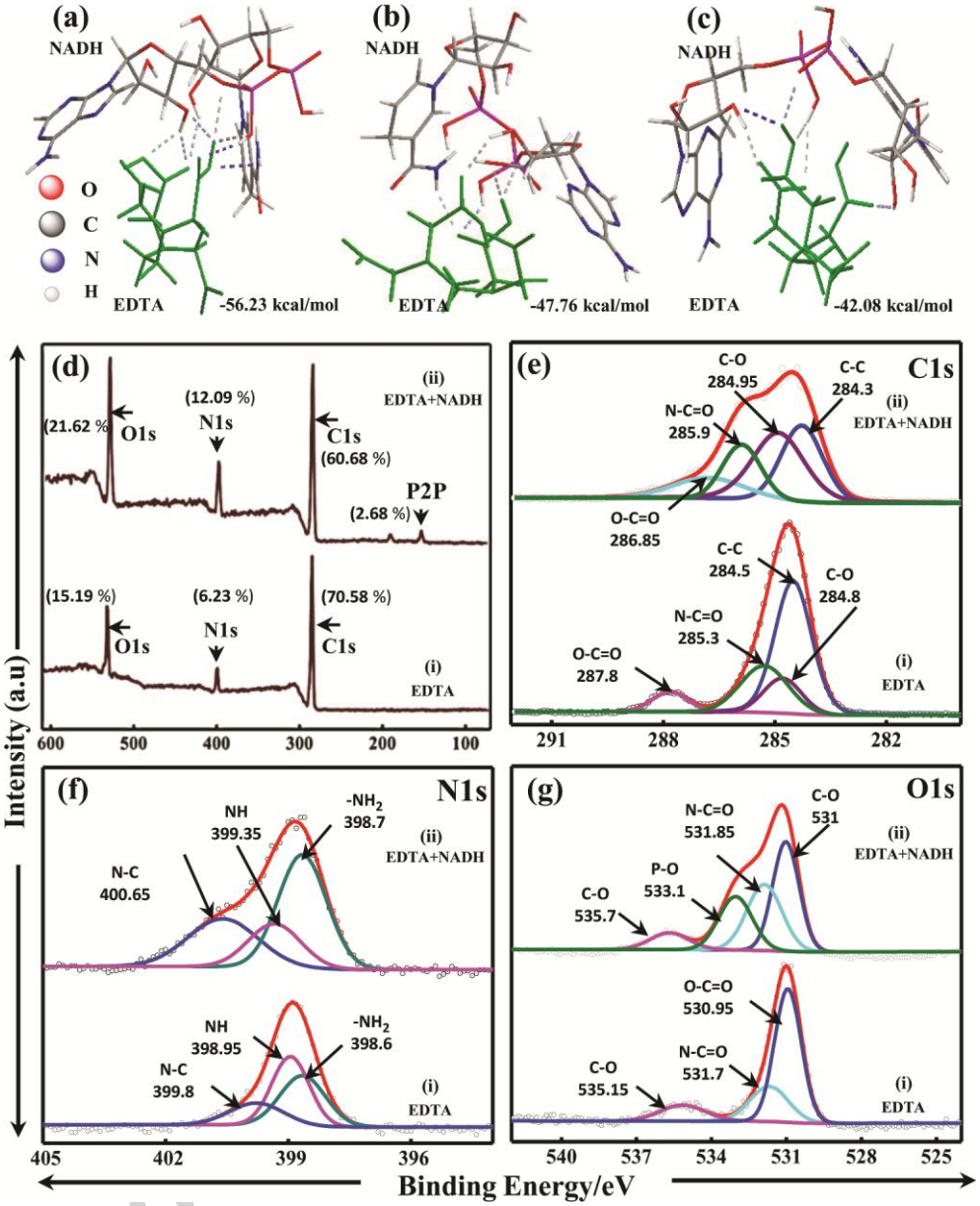
(a)
NADH
O
C
N
H
EDTA
-56.23 kcal/mol
(b)
NADH
EDTA
-47.76 kcal/mol
(c)
NADH
EDTA
-42.08 kcal/mol
(d)
(21.62 %)
O1s
(12.09 %)
N1s
C1s
(60.68 %)
P2P
(2.68 %)
(ii)
EDTA+NADH
(15.19 %)
O1s
(6.23 %)
N1s
C1s
(70.58 %)
(i)
EDTA
600
500
400
300
200
100
(e)
C1s
C-O
284.95
C-C
284.3
N-C=O
285.9
(ii)
EDTA+NADH
O-C=O
286.85
C-C
284.5
C-O
284.8
N-C=O
285.3
O-C=O
287.8
(i)
EDTA
291
288
285
282
Intensity (a.u)
(f)
N1s
NH
399.35
-NH2
398.7
(ii)
EDTA+NADH
N-C
400.65
NH
398.95
-NH2
398.6
N-C
399.8
(i)
EDTA
405
402
399
396
(g)
O1s
N-C=O
531.85
C-O
531
(ii)
EDTA+NADH
P-O
533.1
C-O
535.7
O-C=O
530.95
N-C=O
531.7
C-O
535.15
(i)
EDTA
540
537
534
531
528
525
Binding Energy/eV

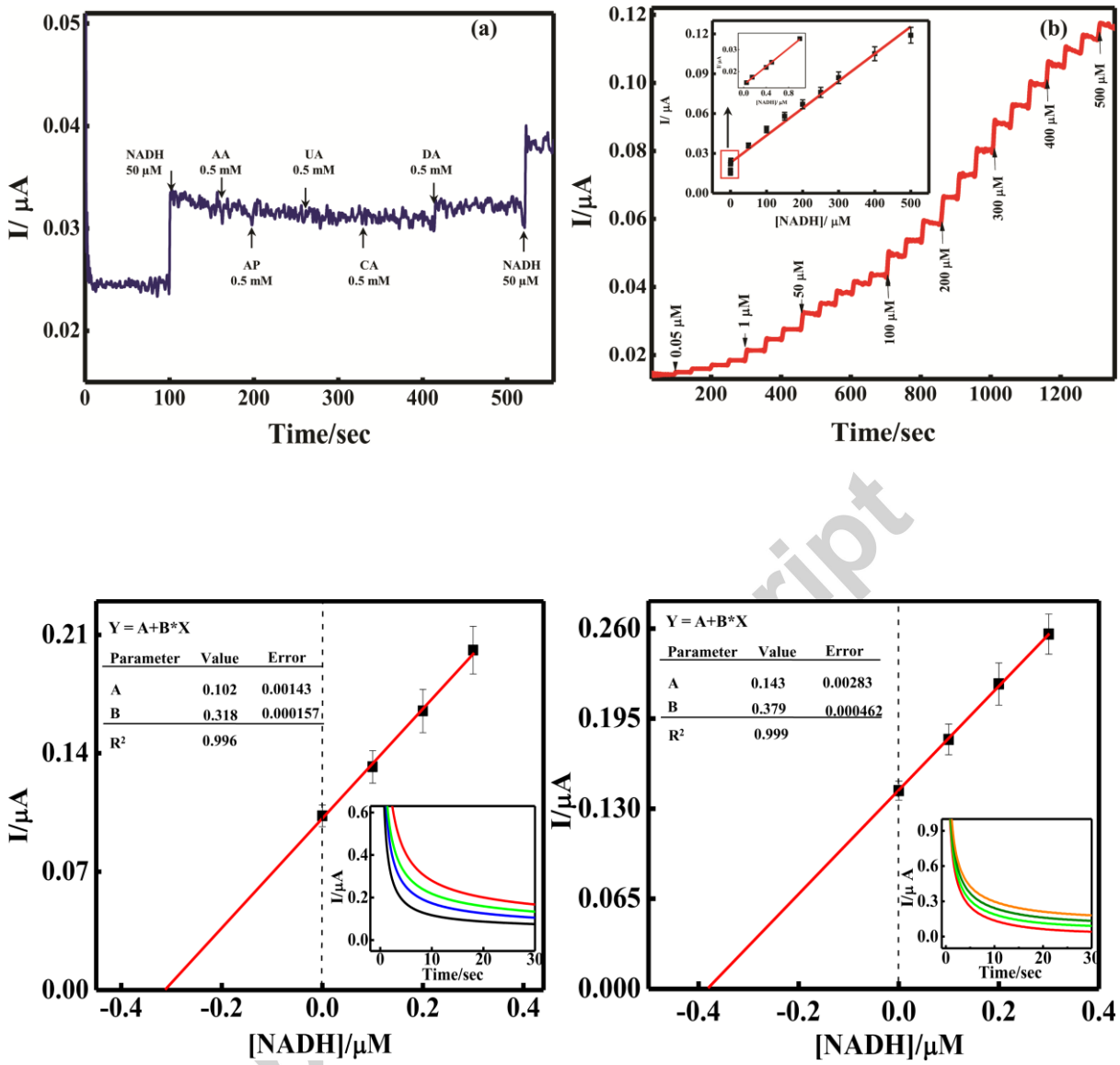

Highlights:

1. A simple, highly sensitive, and selective biosensor was developed for NADH detection using an EDTA complex as probe material.

2. The complex formation between NADH and EDTA molecules was confirmed by estimating the minimized energy, XPS, and QCM.

3. The analytical performance of the proposed sensor was excellent in terms of mitigating the over potential, resistance to fouling, sensitivity, selectivity, and reproducibility.

4. The proposed sensor was successfully applied to detect NADH in human serum and tumorigenic cell samples.